

Direct Numerical Simulations of Turbulent Lifted Hydrogen Jet Flames in Mildly Heated Coflows

Chun Sang Yoo^{1,*}, Jacqueline H. Chen²

¹School of Mechanical and Advanced Materials Engineering, Ulsan National Institute of Science and Technology (UNIST), Ulsan, 689-798, Republic of Korea

²Combustion Research Facility, Sandia National Laboratories, Livermore, CA 945500969, USA

Abstract

Direct numerical simulations (DNSs) of the near field of three-dimensional spatially-developing turbulent hydrogen jet flames in heated coflows at the two intermediate temperatures of 750 and 950 K were performed with a detailed mechanism to elucidate the characteristics of the flame structures and to determine the stabilization mechanism. The DNSs were performed at a jet Reynolds number of 8,000 with 1.28 billion grid points. The results show that relatively-constant low flame speed stabilizes the lifted flame in the coflow of 750 K such that the oscillation of the flamebase is mainly attributed to the passage of large-scale flow structures of the fuel jet. However, for 950 K coflow case high flame speed in hot fuel-lean mixture at the flame base is the main source of the stabilization of the lifted jet flame. Chemical explosive mode analysis (CEMA) and Lagrangian tracking of the flamebase reveal the stabilization mechanisms of the two turbulent jet flames.

1 Introduction

The characteristics of turbulent non-premixed lifted jet flames under various coflow conditions have been widely investigated due to their relevance to practical applications and difficulties to figure out true stabilization mechanisms hidden behind the phenomena.

Numerous studies on stabilization mechanisms of turbulent lifted jet flames have been conducted and various theories regarding the stabilization mechanisms have been proposed. In short, the theories are classified into premixed flame theory, non-premixed flamelet theory, and edge flame theory, based on the premixedness of the mixture. The theories can also be categorized into turbulence intensity theory and large eddy theory, based on the effect of local flow. Readers are referred to reviews by Lyons [1], Pitts [2], and Lawn [3] for more details about the theories.

The stabilization mechanism of turbulent lifted jet flames in hot coflows was studied experimentally and numerically [4-8]. Previous three-dimensional direct numerical simulations (DNS) of hydrogen [4] and ethylene [5] jet flames in highly heated coflow revealed that the turbulent lifted jet flames are stabilized primarily by the auto-ignition of fuel-lean mixtures supported by the hot coflow temperature exceeding the auto-ignition limit and are also determined by the balance between the local axial

velocity and consecutive auto-ignition events occurring in hot fuel-lean mixtures.

However, the stabilization mechanism of turbulent lifted jet flames in mildly-heated coflow, of which temperature is slightly greater or less than the auto-ignition limit, has not been extensively investigated even though overall characteristics of such flames were reported in experimental studies. In this study, therefore, three-dimensional DNSs of turbulent lifted hydrogen jet flames in intermediate-temperature coflows were performed using a detailed hydrogen-air reaction mechanism to understand the stabilization mechanism of turbulent lifted jet flames in mildly heated environment.

The objective of the present DNS study is two-fold: to find stabilization mechanism and structural characteristics of turbulent lifted hydrogen flames in mildly-heated coflows, and to compare the flames with that in highly-heated coflow by examining in detail the instantaneous and time-averaged flame/flow characteristics near the flame base. The role of the near-field, large-scale flow motion in the stabilization mechanism is elucidated by Lagrangian tracking of the flame base together with relevant scalar and velocity fields, similar to the methods developed in the previous study of turbulent lifted jet flames

2 Problem Configuration

The DNSs of turbulent lifted hydrogen jet flames were performed in a three-dimensional slot-burner configuration, which was used for previous studies [4,5]. Diluted hydrogen fuel (65 % hydrogen + 35 % nitrogen by volume) issues from a central jet at an inlet temperature of $T_j = 400$ K. Surrounding the central jet on either side, co-flowing heated air streams issue at $T_c = 750$ K (Case L) and 950 K (Case H) and at atmospheric pressure. The coflow temperatures are high enough to stabilize the flames within the domain but not enough to ignite the mixtures. As such, the mixtures are ignited by high temperature ignition source as in [4]. The mixture composition was selected such that the stoichiometric mixture fraction, $\xi_{st} = 0.1990$, resides in a region of high shear in the developing jet. The fuel jet width, H , is 2 mm and the computational domain is $15H \times 20H \times 3H$ in the streamwise, x , transverse, y , and spanwise, z , directions, which is discretized with $2000 \times 1600 \times 400$ grid points. The mean inlet jet velocity, U_j , and coflow velocity, U_c , are 240 m/s and 2 m/s, respectively such that the Reynolds number based on the fuel jet, Re_j , is 8,000. Readers are referred to Ref. [4,5] for the details of the grid system and turbulence injection methods.

*Corresponding author. Fax: +82-52-217-2309
E-mail address: csyoo@unist.ac.kr

The compressible Navier–Stokes, species continuity, and total energy equations were solved using the Sandia DNS code, S3D [9]. A detailed hydrogen-air kinetic mechanism was adopted [10]. For details of the numerical methods, readers are referred to [9]. Navier–Stokes characteristic boundary conditions (NSCBC) were used to prescribe the boundary conditions [11]. Improved nonreflecting inflow and outflow boundary conditions [12,13] were used in the x - and y -directions, and periodic boundary conditions were applied in the z -direction. Based on the prescribed inlet jet velocity and the streamwise domain length, a flow-through time, $\tau_j (= L_x/U_j)$, is 0.125 ms.

After the ignition by hot source as in [4], lifted jet flame bases approached statistical stationarity and fluctuated about their steady stabilization lift-off heights, h , of approximately $h_L/H = 2.4$ and $h_H/H = 5.3$, where subscripts L and H denote Cases L and H, respectively.

3 Results – Flame Structures

Figure 1 shows the isocontours of the mass fractions of hydroxyl (OH) together with the stoichiometric mixture fraction line at $t/\tau_j = 2.0$ for both cases because hydroxyl has been used as a marker of lifted flamebases or high temperature reaction regions [5-7]. It is readily observed that the reaction zone of Case L is much broader than Case H and the relative location of HO_2 and H_2O_2 has been identified as a measure to determine the characteristics of each lifted flame base [8]. Figure 2 shows that the normalized mass fractions of OH, HO_2 , and H_2O_2 along 1-D lines for Cases L and H. It was found from a previous study [8] that during auto-ignition of H_2/O_2 mixture, HO_2 builds up prior to H_2O_2 and then the other radicals build up, resulting in the thermal run-away. In premixed flames, however, all radicals including HO_2 and H_2O_2 start to increase in the preheat zone nearly at the same location. From Fig. 2, the existence of HO_2 ahead of OH and H_2O_2 in Case H reveals that auto-ignition occurs at the flamebase. In Case L, however, the same radical build-up point (e.g., HO_2 and H_2O_2) verifies that the lifted flame base is a normal premixed flame.

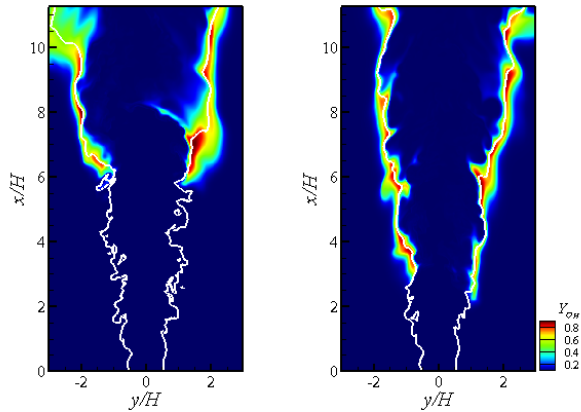


Figure 1. Isocontours of normalized mass fractions of OH at $t/\tau_j = 2$ for Case L (left) and (b) Case H (right) along with the stoichiometric line (white).

To elucidate the stabilization mechanisms of the lifted flames, the global characteristics of the lifted flames are investigated using conditional statistics; the cross-stream conditional Favre mean, $\langle \phi | \eta \rangle$ of a variable, ϕ , where η is the sample space of the mixture fraction, ξ [4,5],

Figures 3 shows $\langle \dot{q} | \eta \rangle$ along the streamwise direction for the two cases. Several points are to be noted from the figure. First,

$\langle \dot{q} | \eta \rangle$ increases first in fuel-lean mixtures in both cases and the

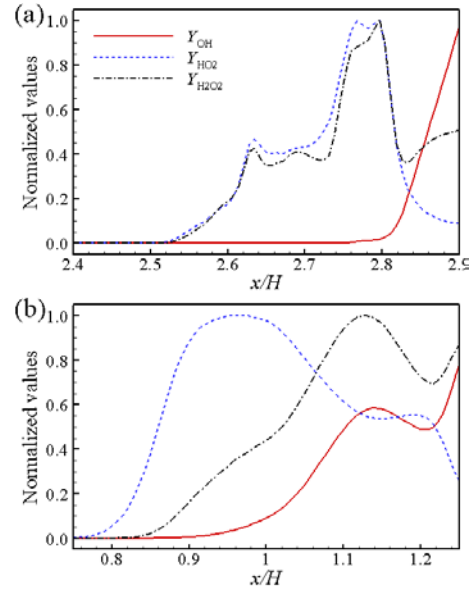


Figure 2. Normalized mass fractions of OH, HO_2 , and H_2O_2 at $t/\tau_j = 2$ for (a) Case L and (b) Case H.

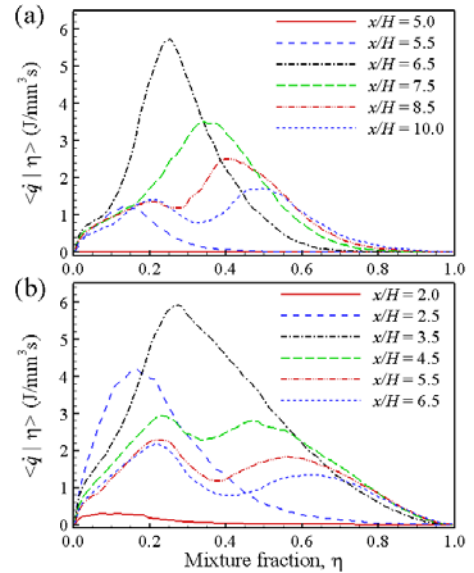


Figure 3. Conditional heat release rate for (a) Case L and (b) Case H.

maximum $\langle \dot{q} | \eta \rangle$ occurs at one jet width downstream of the lift-off height in both cases. It is also observed that the peak $\langle \dot{q} | \eta \rangle$ occurs at stoichiometric to slightly rich conditions within a jet width downstream of the lift-off height and rapidly decreases further downstream. This result implies that for both cases, vigorous reaction occurs within one jet width downstream of the lift-off height. Second, in Case H, relatively large $\langle \dot{q} | \eta \rangle$ occurs in fuel-lean mixture at the lift-off height compared to Case L, implying that high T_c in Case H induces greater heat release at fuel-lean mixtures. Third, in both cases, two peaks in $\langle \dot{q} | \eta \rangle$ form further downstream of the flame base, one centered near the stoichiometric and the other centered in fuel-rich conditions, similar to the result of a previous DNS study [4]. This suggests that the leakage of oxidizer to fuel-rich regions leads to auto-ignition of fuel-rich mixtures.

To further identify the characteristics of the stabilization mechanism, $\langle D\alpha | \eta \rangle$ along the streamwise direction is shown

in Fig. 4 for the two cases. The Damköhler number, Da , is defined as [4,5]:

$$Da = \frac{\dot{\omega}_k}{|-\nabla \cdot (\rho Y_k \mathbf{V}_k)|}, \quad (1)$$

where \mathbf{V}_k and $\dot{\omega}_k$ denote a diffusive velocity vector and a net production rate of species k , respectively. In this study, H_2O is adopted for the Damköhler number analysis. Since Da is defined as the ratio of species reaction term to diffusion, it provides a measure of the local progress of ignition. Therefore, large values of $Da \sim O(\gg 1)$ indicates significant increase of heat and radicals due to ignition.

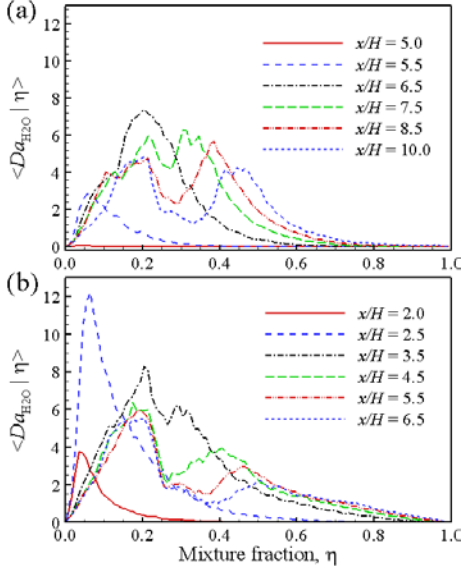


Figure 4. Conditional Damköhler number for (a) Case L and (b) Case H.

It is readily observed from the figure that $\langle Da | \eta \rangle$ exhibits significantly different behavior near the flamebase, which indicates that the two lifted flames may be stabilized by different mechanisms. In Case H, $\langle Da | \eta \rangle$ exhibits large value ($\gg 1$) at fuel-lean mixtures near and upstream of the flame base. In addition, the variance of Da (not shown) is considerably larger than the conditional mean value. This result suggests that the local Da can be significantly larger than unity, and hence, auto-ignition is the main source of stabilization of the lifted flame in Case H. In Case L, however, $\langle Da | \eta \rangle$ is nearly zero upstream of the flamebase and exhibits $O(\sim 1)$ at lean mixtures near the flamebase. In addition, the variance of Da is relatively small compared to that in Case H, suggesting that for Case L, the reaction and diffusion terms balance each other and as such, flame propagation is the stabilization mechanism of the lifted flame.

4 Results – Chemical Explosive Mode

Chemical explosive mode analysis (CEMA) is adopted to further identify the characteristics of the lifted flamebases [5,14]. The method of CEMA is briefly introduced here. The differential equations of a typical reacting flow can be described in discretized form as:

$$\frac{D\mathbf{y}}{Dt} = \mathbf{g}(\mathbf{y}) = \boldsymbol{\omega}(\mathbf{y}) + \mathbf{s}(\mathbf{y}), \quad (2)$$

where D/Dt is the material derivative and \mathbf{y} is the solution vector including species concentrations and temperature. $\boldsymbol{\omega}$ and \mathbf{s} represent, respectively, the chemical source term and all

non-chemical terms such as diffusion and homogeneous mixing.

The Jacobian matrix of the chemical source term, \mathbf{J}_ω ($\equiv \partial \boldsymbol{\omega} / \partial \mathbf{y}$), can fully describe the local chemical information such that a chemical mode can be defined as an eigenmode of \mathbf{J}_ω , which is associated with an eigenvalue and a corresponding pair of the left and right eigenvectors. CEM is defined as a chemical mode of which real part of the eigenvalue, λ_e , is positive. CEM represents the reciprocal chemical time scale of a local mixture and as such, the existence of CEM implies that the corresponding mixture is explosive in nature. It is, therefore, apt to auto-ignite when the mixture resides in a lossless environment with negligible \mathbf{s} in Eq. (2). However, a mixture exhibiting CEM does not necessarily lead to thermal run-away if the mixture significantly loses heat and radicals. Therefore, CEM is an intrinsic characteristic of ignitable mixtures.

In nonpremixed turbulent flames, the loss of heat and radicals can be characterized by the mixing or scalar dissipation rate, χ , which is defined by $\chi = 2D|\nabla \xi|^2$, where D is a local thermal diffusivity. The competition between the CEMs and the losses can be approximately be quantified by a Damköhler number defined by $Da_c = \lambda_e \cdot \chi^{-1}$. Note that a mixture with $Da_c \gg 1$ indicates a dominant CEM which will be likely to result in actual ignition; otherwise ignition may be suppressed by the losses.

Figure 5 shows the isocontours of Da_c for the two cases. Several points are to be noted. First, for both cases, a large positive Da_c in red indicates that the CEM dominates the mixing process such that the mixture is auto-igniting. A large negative Da_c in blue, however, indicates a fast reacting post-ignition mixture such that its overall reaction progress can be limited by the slower local transport process. As such, the dark blue regions in Fig. 5 contain diffusion flame kernels. Second, for Case H, two strips of auto-igniting mixtures (red) upstream of the flamebase can be readily observed in Fig. 5b, leading to ignited mixtures (blue). This result verifies that the stabilization mechanism of Case H is auto-ignition. In Case L, however, a large positive Da_c occurs only at narrow regions upstream of the flamebase, which must be the preheated zone of a premixed flame, considering the coflow temperature of Case L.

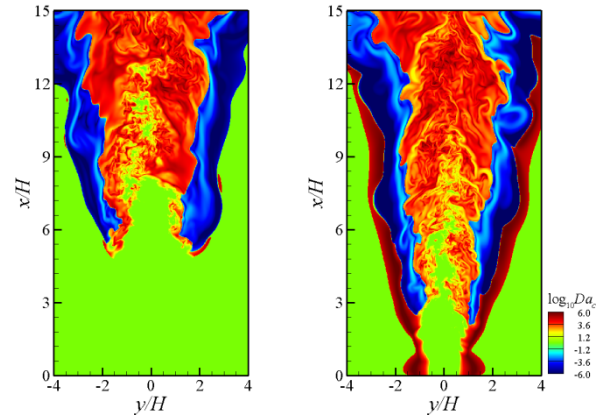


Figure 5. Isocontours of Da_c at $t/\tau_j = 2$ for Case L (left) and (b) Case H (right).

5 Results – Flamebase Dynamics

The characteristics of the stabilization point movement are investigated by correlating with other key scalar quantities and velocity. The temporal evolution of the stabilization point along with flame-normal flow velocity ($\mathbf{u} \cdot \mathbf{n}$), displacement speed (S_d), mixture fraction (ξ), and scalar dissipation rate (χ) at the

$z = 0$ plane are presented in Figs. 6 and 7. All values are evaluated at the stabilization point of each flame. The displacement speed of species k , S_d , is defined as:

$$S_d = \frac{1}{\rho |\nabla Y_k|} (\dot{\omega}_k - \nabla \cdot (\rho Y_k \mathbf{V}_k)). \quad (3)$$

The hydroxyl iso-surface associated with the stabilization point, $Y_{OH} = 0.001$, is used to evaluate the displacement speed [4,5].

Lagrangian tracking of the flamebase of 950 K coflow case reveals that S_d at the flamebase exhibits sporadically large positive (> 20 m/s) and negative values as shown in Fig. 6, resulting in a “hanging chain” shaped movement of the flamebase, which is qualitatively similar to that of the previous hydrogen jet flame [4]. The large positive and negative S_d of the flamebase indicates that the auto-ignition is the main source of stabilization. Note that the laminar flame speed $\xi = 0.05$ of the flame is approximately 2 m/s.

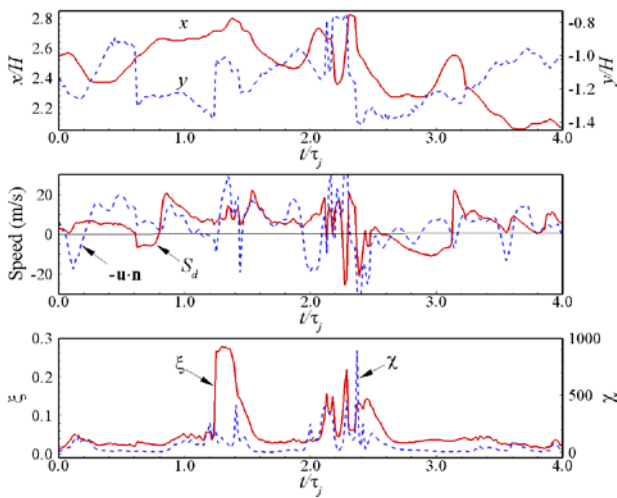


Figure 6. Temporal evolution of key scalar variables at the stabilization point at $z = 0$ for Case H.

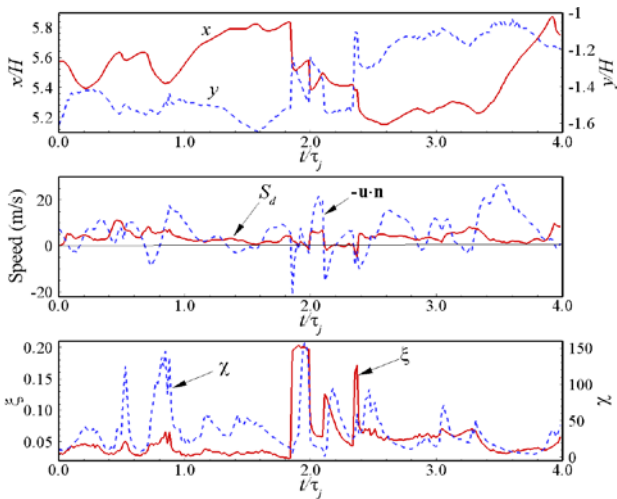


Figure 7. Temporal evolution of key scalar variables at the stabilization point at $z = 0$ for Case L.

On the contrary, S_d of 750 K coflow is nearly always positive and exhibits smaller value ($\bar{S}_d \sim 3.6$ m/s) compared to the large local velocity as shown in Fig. 7(b). This implies that the flame propagation is the main source of stabilization and the flamebase movement is more apt to depend on local velocity.

From Fig. 7, the mean local velocity is found to be

approximately 5.9 m/s at the flamebase, which is quite comparable to \bar{S}_d of the flamebase such that the flamebase is stabilized at which the mean propagation speed of the flamebase balances the mean local velocity normal to the flame surface at the flamebase.

6 Conclusions

Three-dimensional DNSs of the near field of turbulent hydrogen slot-burner jet flames in an auto-igniting ($T_c = 950$ K) and a non-igniting ($T_c = 750$ K) heated coflows were performed with a detailed mechanism and mixture-averaged transported properties. The spatial order of intermediate species, the conditional mean of Damköhler number, and chemical explosive mode analysis show that the lifted flame with high coflow temperature is mainly stabilized by the auto-ignition of the lean mixtures in low scalar dissipation rate region. However, the stabilization mechanism of the lifted flame with low coflow temperature is the flame propagation of the lean mixtures under low scalar dissipation rate and relatively high temperature region.

Lagrangian tracking of the flamebase reveals that relatively-constant low flame speed stabilizes the lifted flame in the coflow of 750 K such that the oscillation of the flamebase is mainly attributed to the passage of large-scale flow structures of the fuel jet. For the case with 950 K coflow, auto-ignition and flame propagation with high flame speed in hot fuel-lean mixture is the main source of stabilization of the lifted jet flame.

7 Acknowledgments

This work was supported by Basic Science Research Program through the National Research Foundation of Korea (NRF) funded by the Ministry of Education, Science and Technology (No. 2012-0003222). This research used the resources of the National Center for Computational Sciences at Oak Ridge National Laboratory.

References

- [1] K.M. Lyons, *Prog. Energy Combust. Sci.* 33 (2007) 211–231.
- [2] W.M. Pitts, *Proc. Combust. Inst.* 22 (1998) 809–816.
- [3] C.J. Lawn, *Prog. Energy Combust. Sci.* 35 (2009) 1–30.
- [4] C.S. Yoo, R. Sankaran, J.H. Chen, *J. Fluid Mech.* 640 (2009) 453–481.
- [5] C.S. Yoo, E.S. Richardson, R. Sankaran, J.H. Chen, *Proc. Combust. Inst.* 33 (2011) 1619–1627.
- [6] R. Cabra, T. Myhrvold, J.Y. Chen, R.W. Dibble, A.N. Karpets, R.S. Barlow, *Proc. Combust. Inst.* 29 (2002) 1881–1888.
- [7] J.E. Dec, *SAE Trans.* 105 (1997) 1319–1348.
- [8] R.L. Gordon, A.R. Masri, S.B. Pope, G.M. Goldin, *Combust. Theory Modelling* 11 (2007) 351–376.
- [9] J.H. Chen et al., *Comput. Sci. Disc.* 2 (2009) 015001.
- [10] J. Li, Z. Zhao, A. Kazakov, F.L. Dryer, *Int. J. Chem. Kinet.* 36 (2004) 566–575.
- [11] T.J. Poinsot, S.K. Lele, *J. Comput. Phys.* 101 (1992) 104–139.
- [12] C.S. Yoo, Y. Wang, A. Trouvé, H.G. Im, *Combust. Theory Modelling* 9 (2005) 617–646.
- [13] C.S. Yoo, H.G. Im, *Combust. Theory Modelling* 11 (2007) 259–286.
- [14] T. Lu, C.S. Yoo, J.H. Chen, C.K. Law, *J. Fluid Mech.* 652 (2010) 45–64.